IOP Publishing Inverse Problems

Inverse Problems **33** (2017) 125016 (28pp) https://doi.org/10.1088/1361-6420/aa9909

A general approach to regularizing inverse problems with regional data using Slepian wavelets*

Volker Michel[1] **and Frederik J Simons**[2]

[1] Department of Mathematics, Geomathematics Group, University of Siegen, Germany
[2] Department of Geosciences, Guyot Hall, Princeton University, NJ, United States of America

E-mail: michel@mathematik.uni-siegen.de and fjsimons@alum.mit.edu

Received 4 August 2017, revised 30 October 2017
Accepted for publication 8 November 2017
Published 30 November 2017

Abstract

Slepian functions are orthogonal function systems that live on subdomains (for example, geographical regions on the Earth's surface, or bandlimited portions of the entire spectrum). They have been firmly established as a useful tool for the synthesis and analysis of localized (concentrated or confined) signals, and for the modeling and inversion of noise-contaminated data that are only regionally available or only of regional interest. In this paper, we consider a general abstract setup for inverse problems represented by a linear and compact operator between Hilbert spaces with a known singular-value decomposition (svd). In practice, such an svd is often only given for the case of a global expansion of the data (e.g. on the whole sphere) but not for regional data distributions. We show that, in either case, Slepian functions (associated to an arbitrarily prescribed region and the given compact operator) can be determined and applied to construct a regularization for the ill-posed regional inverse problem. Moreover, we describe an algorithm for constructing the Slepian basis via an algebraic eigenvalue problem. The obtained Slepian functions can be used to derive an svd for the combination of the regionalizing projection and the compact operator. As a result, standard regularization techniques relying on a known svd become applicable also to those inverse problems where the data are regionally given only. In particular, wavelet-based multiscale techniques can be used. An example for the latter case is elaborated theoretically and tested on two synthetic numerical examples.

* www.geomathematics-siegen.de and www.frederik.net

1361-6420/17/125016+28$33.00

Keywords: ill-posed problem, inverse problem, regional data, regularization, singular-value decomposition, Slepian function, wavelet

(Some figures may appear in colour only in the online journal)

1. Introduction

In a wide range of scientific applications, concentrated in but not confined to the geosciences, regional modelling from global data has become increasingly important, for a variety of reasons. For example, regional phenomena like the melting of the Greenland or Antarctica ice sheets are being studied on the basis of global satellite (potential-field, e.g. gravity) data [18]. Alternatively, geophysical data could be of regionally varying quality, either in terms of their measurement density, or owing to spatial variations in signal-to-noise ratios. Finally, localization and regionalization may be part of a strategy to 'divide and conquer' data domains, which is often a necessity for solving the kinds of problems that involve the large data volumes with which the geosciences are routinely confronted.

In this general context [9], the use of localized trial functions has proven to be useful. One among the many ways by which such Ansatz functions can be constructed, the idea behind the 'Slepian' approach is as follows. Taking R to be a subdomain, a portion of a complete domain D (e.g. an interval on the set of real numbers, or a spherical cap on the surface of a ball), we determine the function F that maximizes the fraction

$$\lambda := \frac{\int_R [F(x)]^2 \,\mathrm{d}x}{\int_D [F(x)]^2 \,\mathrm{d}x}, \tag{1}$$

the quotient of the squared L^2-norms of F on R and on D. For practical purposes, the choice of F is restricted to a finite-dimensional space. This is achieved, for example, by assuming a bandlimit for F. The first notions of Slepian functions treated the case of the real line, and appeared in the literature in the early 1960s, in the work by [22, 38, 39], who were concerned with problems in communication theory. In the late 1990s, Slepian functions on the sphere were derived for use in geodesy and planetary science [2, 4, 34–36, 44, 45]. In parallel, a few alternative approaches, using different measures of optimality, have been developed for constructing approximating structures on the sphere, see, for example, [20, 21, 24].

If D is the 2-sphere, the functions F can be expanded in the well-known $\mathrm{L}^2(D)$-orthonormal system of spherical harmonics $Y_{l,m}$ of degree l and order m (see e.g. [7, 25, 27]) up to a fixed maximal degree L,

$$F(\xi) = \sum_{l=0}^{L} \sum_{m=-l}^{l} \langle F, Y_{l,m} \rangle_{\mathrm{L}^2} Y_{l,m}(\xi), \quad |\xi| = 1.$$

The maximization problem (1) leads to an algebraic eigenvalue problem, whose eigenvectors are vectors with the expansion coefficients of F in the chosen basis (in the above case, the $Y_{l,m}$), and whose eigenvalues are the ratios λ in (1). Since the corresponding matrix is Gramian and, therefore, symmetric, an orthonormal basis of eigenvectors spanning the entire space of possible expansion coefficient vectors can be found. Owing to Parseval's identity, the functions that correspond to the expansion coefficient vectors also constitute an orthonormal basis for the (bandlimited) space of considered functions. As a consequence, the previously used basis can be replaced by a new basis, the 'Slepian' basis, whose elements are sorted according to their localization λ over the subdomain R. This new basis is also orthogonal in the sense of $\mathrm{L}^2(R)$, which simplifies the expansion of bandlimited signals that are restricted to the subdomain R.

Recently, Slepian functions have revealed themselves to be also useful for the regularization of inverse problems in geophysics. For example, [29] addressed the downward continuation of a gravity or magnetic field from regionally given gradients of the potential at satellite altitude. Using $\mathcal{T}F = G$ to represent the inverse problem, involving an operator $\mathcal{T}$, a given function G, and an unknown function F, [29] constructed Slepian basis functions via the maximization of

$$\tilde{\lambda} := \frac{\int_R [\mathcal{T}F(x)]^2 \, \mathrm{d}x}{\int_D [F(x)]^2 \, \mathrm{d}x}. \tag{2}$$

Here, R need not be a subset of D any more, but, rather, is the domain of functions in the range of $\mathcal{T}$. In the particular case considered by [29], R is a region at satellite altitude where data are being collected, and D represents the (spherical) Earth's surface.

In this paper, we will show that equations (1) and (2) can be seen as particular examples of a more general approach to the construction of Slepian functions for inverse problems. In particular, in the typical application scenario, one has an inverse problem $\mathcal{T}F = G$ for which an svd is known if and when G is given on a domain $\tilde{D}$. When G is only given on a subdomain $R \subset \tilde{D}$, we show that Slepian functions can be used to derive an svd also for the restricted case $\mathcal{P}\mathcal{T}F = G|_R$, with a corresponding projection operator $\mathcal{P}$. The knowledge of such an svd opens the door to various established regularization methods.

To the knowledge of the authors, there are only a few other publications which use Slepian functions for inverse problems. For example, another approach which addresses the singular-value decomposition of the operator is developed in [17] for functions on the real line and a particular integral operator. Moreover, in [1], the gravitational potential is expanded in spherical Slepian functions. The result is used as the given right-hand side for an inverse problem, where point masses are reconstructed which approximately generate the corresponding regional gravitational potential. Examples in other application domains are [6, 15, 26, 33].

Other systems of localized trial functions have been used for inverse problems as well. This includes, in particular, wavelet methods [11]. It would be beyond the scope and size of this article to give a complete survey of such papers here. Examples of other works where wavelets have been used for inverse problems on the sphere are [13, 37, 40, 43]. In [8, 23] it was shown that a wavelet-based regularization can be constructed if the svd of the forward operator is known. Therefore, we use these latter papers as a motivation for establishing a Slepian-based wavelet method for inverse problems with regional data.

The outline of this paper is as follows: in section 2, we introduce some basic notation. The general setup of a linear compact operator between two Hilbert spaces is described in section 3. For this scenario, we explain the construction of Slepian functions in section 4. Since the general setting includes also infinite-dimensional spaces but numerical implementations are only possible for finite dimensions, the practical specifics are discussed in section 5. Since the setting of [29] also includes an inverse problem where data originating from two different kinds of sources are being inverted, we show in section 6 how such coupled problems can be integrated into the general scenario. In section 7 we describe an algorithm for determining the Slepian functions and calculating the svd of the restricted (projected) forward operator. Motivated by some known results for Slepian functions on particular domains, we show in section 8 how Slepian functions can be used to establish Fredholm integral operators for the forward and the inverse operator. In particular, we also show how scaling functions and wavelets can be constructed from the Slepian functions, and we prove convergence and stability of the method. This multiscale regularization technique is then applied to two inverse problems and tested numerically for synthetic data sets in section 9. Finally, in section 10, we offer conclusions and an outlook on future research.

2. Notation

As usual, $\mathbb{N}$ represents the set of all positive integers, where $\mathbb{N}_0 := \mathbb{N} \cup \{0\}$, and $\mathbb{R}$ and $\mathbb{C}$ stand for the fields of all real and complex numbers, respectively. A 2-sphere with radius $r > 0$ in $\mathbb{R}^3$ and centre 0 is denoted

$$\Omega_r := \left\{ \xi \in \mathbb{R}^3 \,\middle|\, |\xi| = r \right\}.$$

We write $\Omega := \Omega_1$ for the unit sphere, $r = 1$. Moreover, if $D \subset \mathbb{R}^n$ is measurable, then $\mathrm{L}^2(D)$ is the Hilbert space of square-integrable functions, where almost everywhere equal functions are collected in equivalence classes.

3. Setting

As we mentioned in the Introduction, we will present a general setup for Slepian functions. For this purpose, we introduce here an abstract setting which will serve as a starting point. We have three non-trivial Hilbert spaces $(\mathcal{X}, \langle\cdot,\cdot\rangle_{\mathcal{X}})$, $(\mathcal{Y}, \langle\cdot,\cdot\rangle_{\mathcal{Y}})$, and $(\mathcal{Z}, \langle\cdot,\cdot\rangle_{\mathcal{Z}})$, with the following additional assumptions.

- There exists an isometric embedding (an injection) $\iota : \mathcal{Z} \hookrightarrow \mathcal{Y}$, i.e.

$$\langle \iota(F_1), \iota(F_2) \rangle_{\mathcal{Y}} = \langle F_1, F_2 \rangle_{\mathcal{Z}} \quad \text{for all } F_1, F_2 \in \mathcal{Z}. \tag{3}$$

  We, therefore, consider $\mathcal{Z}$ to be a subset of $\mathcal{Y}$ by associating $\mathcal{Z}$ with $\iota(\mathcal{Z})$. Since ι is isometric and $(\mathcal{Z}, \langle\cdot,\cdot\rangle_{\mathcal{Z}})$ is a Hilbert space, also $(\iota(\mathcal{Z}), \langle\cdot,\cdot\rangle_{\mathcal{Y}})$ is a Hilbert space, namely, a Hilbert subspace of $(\mathcal{Y}, \langle\cdot,\cdot\rangle_{\mathcal{Y}})$.
- There exists a projection $\mathcal{P} : \mathcal{Y} \to \mathcal{Z}$, in the sense that (with '$\mathcal{Z} \subset \mathcal{Y}$')

$$\mathcal{P}(\mathcal{P}G) = \mathcal{P}G \quad \text{for all } G \in \mathcal{Y},$$

  such that $\mathcal{P} \circ \iota = \mathrm{Id}_{\mathcal{Z}}$, in other words, $\mathcal{P}$ inverts the embedding.

For a better understanding, we discuss an example of an application.

Example 3.1. A typical challenging inverse problem in the geosciences is the downward continuation problem (see e.g. [3, 5, 10, 14, 28, 30, 31, 41, 42]). As considered by [29], a harmonic potential (e.g. the gravitational or magnetic potential) is given on a sphere with radius r_{s} (e.g. the satellite orbit), and the task is to determine the potential on the surface of the planet (a sphere with radius r_{p}). In this case, we might choose

$$\mathcal{X} = \mathrm{L}^2\left(\Omega_{r_{\mathrm{p}}}\right), \quad \mathcal{Y} = \mathrm{L}^2\left(\Omega_{r_{\mathrm{s}}}\right), \quad \mathcal{Z} = \mathrm{L}^2(R)$$

as spaces where $R \subset \Omega_{r_{\mathrm{s}}}$ is a subdomain, also a 2-dimensional surface. For example, R could be an area of limited access by measurement, or to which the analysis of the potential is restricted. The canonical embedding would then be $\iota : \mathrm{L}^2(R) \hookrightarrow \mathrm{L}^2(\Omega_{r_{\mathrm{s}}})$ with

$$[\iota(F)](x) := \begin{cases} F(x), & x \in R \\ 0, & x \notin R \end{cases}, \qquad x \in \Omega_{r_{\mathrm{s}}}.$$

It is clear that, for real $F_1, F_2 \in \mathrm{L}^2(R)$, we have

$$\begin{aligned}\langle \iota(F_1), \iota(F_2)\rangle_{\mathrm{L}^2(\Omega_{r_\mathrm{s}})} &= \int_{\Omega_{r_\mathrm{s}}} [\iota(F_1)](\xi)\ [\iota(F_2)](\xi)\,\mathrm{d}\omega(\xi)\\ &= \int_R F_1(\xi)\,F_2(\xi)\,\mathrm{d}\omega(\xi)\\ &= \langle F_1, F_2\rangle_{\mathrm{L}^2(R)}\ .\end{aligned}$$

The projection $\mathcal{P} : \mathrm{L}^2(\Omega_{r_\mathrm{s}}) \to \mathrm{L}^2(R)$ would simply be the restriction

$$\mathcal{P} : G \mapsto G|_R\ .$$

It is similar to the restriction operator used in [36, their equation (4.22)].

Let us return to the general setting again.

Lemma 3.2. *We have*

$$\iota \circ \mathcal{P}|_{\iota(\mathcal{Z})} = \mathrm{Id}_{\iota(\mathcal{Z})},$$

and $\iota \circ \mathcal{P}$ is a projection onto $\iota(\mathcal{Z})$.

This lemma easily follows from the required properties above.

We will now continue with the abstract setting for the inverse problem. For this purpose, we also assume that we have a compact operator $\mathcal{T} : \mathcal{X} \to \mathcal{Y}$ with a known svd

$$\mathcal{T}F = \sum_n \sigma_n \langle F, u_n\rangle_{\mathcal{X}}\, v_n, \quad F \in \mathcal{X}, \tag{4}$$

where $(\sigma_n)_n \subset \mathbb{C}$ satisfies $\sigma_n \neq 0$ for all n. Moreover, as usual for an svd, $(u_n)_n$ and $(v_n)_n$ are orthonormal systems in $\mathcal{X}$ and $\mathcal{Y}$, respectively.

Furthermore, we have an inverse problem $\mathcal{T}F = \tilde{G}$, where $\tilde{G} \in \mathcal{Y}$ is given and $F \in \mathcal{X}$ is unknown. In our case, we assume that $\tilde{G} \in \iota(\mathcal{Z})$, which might mean there is an original and unknown 'whole' signal $G_{\text{whole}} \in \mathcal{Y}$, of which only the partial information $\mathcal{P}G_{\text{whole}} \in \mathcal{Z}$ is given such that $\tilde{G} = \iota\mathcal{P}G_{\text{whole}}$. For these reasons, we will deal here with the inverse problem

$$\mathcal{P}\mathcal{T}F = G, \quad G \in \mathcal{Z} \text{ given}, \ F \in \mathcal{X} \text{ unknown}.$$

Unfortunately, we have the svd for the operator $\mathcal{T} : \mathcal{X} \to \mathcal{Y}$, but not for the operator $\mathcal{P}\mathcal{T} : \mathcal{X} \to \mathcal{Z}$. As we will see, the basic principle of a Slepian approach is to obtain an svd for $\mathcal{P}\mathcal{T}$, which is useful in cases where data are only obtainable from $\mathcal{Z}$.

Example 3.3. We continue with the inverse problem from Example 3.1, the downward continuation problem of [29]. The forward operator $\mathcal{T} : \mathrm{L}^2(\Omega_{r_\mathrm{p}}) \to \mathrm{L}^2(\Omega_{r_\mathrm{s}})$ has the svd

$$\mathcal{T}F = \sum_{l=0}^{\infty} \sum_{m=-l}^{l} \left(\frac{r_\mathrm{p}}{r_\mathrm{s}}\right)^l \left\langle F, \frac{1}{r_\mathrm{p}} Y_{l,m}\left(\frac{\cdot}{r_\mathrm{p}}\right)\right\rangle_{\mathrm{L}^2(\Omega_{r_\mathrm{p}})} \frac{1}{r_\mathrm{s}} Y_{l,m}\left(\frac{\cdot}{r_\mathrm{s}}\right),$$

for $F \in \mathrm{L}^2(\Omega_{r_\mathrm{p}})$, where $(Y_{l,m})_{l\in\mathbb{N}_0;\, m=-l,\ldots,l}$ is the commonly used orthonormal basis of real spherical harmonics in $\mathrm{L}^2(\Omega)$. Here, $R \subset \Omega_{r_\mathrm{s}}$ is the subdomain of data availability, or of modeling interest for the potential. Moreover, r_s (radius of e.g. the satellite orbit) is larger than r_p (radius of the surface of the planet).

4. Slepian approach

In analogy with [29], we pursue the idea to maximize

$$\mathcal{R}(F) := \frac{\|\mathcal{P}\mathcal{T}F\|_{\mathcal{Z}}^2}{\|F\|_{\mathcal{X}}^2} \tag{5}$$

among all $F \in \mathcal{X}$ with $F \neq 0$. The individual terms can be represented as follows ($\mathcal{P}_{\ker \mathcal{T}}$ is the orthogonal projection onto the nullspace or kernel of $\mathcal{T}$), for $F \in \mathcal{X}$,

$$\begin{aligned}
\|F\|_{\mathcal{X}}^2 &= \sum_n |\langle F, u_n\rangle_{\mathcal{X}}|^2 + \|\mathcal{P}_{\ker \mathcal{T}} F\|_{\mathcal{X}}^2 ,\\
\mathcal{T}F &= \sum_n \sigma_n \langle F, u_n\rangle_{\mathcal{X}}\, v_n,\\
\mathcal{P}\mathcal{T}F &= \sum_n \sigma_n \langle F, u_n\rangle_{\mathcal{X}}\, \mathcal{P}v_n,\\
\|\mathcal{P}\mathcal{T}F\|_{\mathcal{Z}}^2 &= \sum_{m,n} \sigma_m \overline{\sigma_n} \langle F, u_m\rangle_{\mathcal{X}} \overline{\langle F, u_n\rangle_{\mathcal{X}}} \langle \mathcal{P}v_m, \mathcal{P}v_n\rangle_{\mathcal{Z}}.
\end{aligned} \tag{6}$$

Note that these formulae are also valid if $(v_n)_n$ is *not* orthonormal in $\mathcal{Y}$. It suffices that (4), which is the same as (6), is a finite sum or a (strongly) convergent series.

Example 4.1. Let us consider again Example 3.3. In this case, the kernel is trivial, i.e. $\ker \mathcal{T} = \{0\}$. Furthermore,

$$\begin{aligned}
\|F\|_{\mathrm{L}^2(\Omega_{r_\mathrm{p}})}^2 &= \sum_{l=0}^{\infty} \sum_{m=-l}^{l} \left\langle F, \frac{1}{r_\mathrm{p}} Y_{l,m}\left(\frac{\cdot}{r_\mathrm{p}}\right)\right\rangle_{\mathrm{L}^2(\Omega_{r_\mathrm{p}})}^2 ,\\
\|\mathcal{P}\mathcal{T}F\|_{\mathrm{L}^2(R)}^2 &= \sum_{l=0}^{\infty} \sum_{m=-l}^{l} \sum_{l'=0}^{\infty} \sum_{m'=-l'}^{l'} \left(\frac{r_\mathrm{p}}{r_\mathrm{s}}\right)^{l+l'} \left\langle F, \frac{1}{r_\mathrm{p}} Y_{l,m}\left(\frac{\cdot}{r_\mathrm{p}}\right)\right\rangle_{\mathrm{L}^2(\Omega_{r_\mathrm{p}})}\\
&\quad \times \left\langle F, \frac{1}{r_\mathrm{p}} Y_{l',m'}\left(\frac{\cdot}{r_\mathrm{p}}\right)\right\rangle_{\mathrm{L}^2(\Omega_{r_\mathrm{p}})}\\
&\quad \times \int_R \frac{1}{r_\mathrm{s}} Y_{l,m}\left(\frac{\eta}{r_\mathrm{s}}\right) \frac{1}{r_\mathrm{s}} Y_{l',m'}\left(\frac{\eta}{r_\mathrm{s}}\right) \mathrm{d}\omega(\eta).
\end{aligned}$$

Lemma 4.2. *The ratio $\mathcal{R}$, which was defined in (5), satisfies*

$$0 \leqslant \mathcal{R}(F) \leqslant \max_n |\sigma_n|^2$$

for all $F \in \mathcal{X} \setminus \{0\}$.

Proof. Since $\mathcal{P}$ is a projection, its operator norm must satisfy $\|\mathcal{P}\|_{\mathcal{L}(\mathcal{Y},\mathcal{Z})} = 1$. Moreover, the singular-value decomposition (4) yields that $\|\mathcal{T}\|_{\mathcal{L}(\mathcal{X},\mathcal{Y})} = \max_n |\sigma_n|$. Note that this maximum exists, since $\mathcal{T}$ is compact and, therefore, $(\sigma_n)_n$ must either be a finite sequence or a sequence which converges to zero. Hence, $\|\mathcal{P}\mathcal{T}\|_{\mathcal{L}(\mathcal{X},\mathcal{Z})} \leqslant \max_n |\sigma_n|$, where

$$\|\mathcal{P}\mathcal{T}\|_{\mathcal{L}(\mathcal{X},\mathcal{Z})}^2 = \sup_{F\in\mathcal{X}\setminus\{0\}} \mathcal{R}(F).$$

□

Lemma 4.3. *The operator $\mathcal{PT} : \mathcal{X} \to \mathcal{Z}$ is compact.*

Proof. $\mathcal{T}$ is compact and $\mathcal{P}$ is (as every projection) continuous. Hence, $\mathcal{PT}$ is compact. □

As a consequence, $\mathcal{PT}$ must have a singular-value decomposition

$$\mathcal{PT}F = \sum_n \tau_n \langle F, g_n \rangle_{\mathcal{X}} \, h_n, \quad F \in \mathcal{X}, \tag{7}$$

where $(\tau_n)_n \subset \mathbb{C}$ is either a finite sequence or a sequence converging to zero, $(g_n)_n$ is an orthonormal system in $\mathcal{X}$, and $(h_n)_n$ is an orthonormal system in $\mathcal{Z}$. We will assume here that the singular values $(\tau_n)_n$ are sorted in a way such that $(|\tau_n|)_n$ is monotonically decreasing. The corresponding sequence $(g_n)_n$ will be called a sequence of *Slepian basis functions* with a localization[3] of descending order. This is motivated by the fact that

$$\mathcal{R}(g_n) = \frac{\|\mathcal{PT}g_n\|_{\mathcal{Z}}^2}{\|g_n\|_{\mathcal{X}}^2} = |\tau_n|^2. \tag{8}$$

5. Finite-dimensional case

In numerical implementations, only finite basis systems can be used. This usually means that the analysis is restricted to bandlimited functions. Because of its practical relevance, we discuss this particular case here separately. We set

$$f := (\langle F, u_n \rangle_{\mathcal{X}})_{n=1,\dots,N} \in \mathbb{C}^N \quad \text{(column vector)},$$

$$\Sigma := \begin{pmatrix} \sigma_1 & 0 & \cdots & 0 \\ 0 & \ddots & \ddots & \vdots \\ \vdots & \ddots & \ddots & 0 \\ 0 & \cdots & 0 & \sigma_N \end{pmatrix} \in \mathbb{C}^{N\times N},$$

$$K := (\langle \mathcal{P}v_m, \mathcal{P}v_n \rangle_{\mathcal{Z}})_{m,n=1,\dots,N} \in \mathbb{C}^{N\times N}.$$

Then the Parseval identity implies that

$$\mathcal{R}(F) = \|f\|_{\mathbb{C}^N}^{-2} \cdot f^{\mathrm{T}} \Sigma K \Sigma^* \overline{f}.$$

Here, M^* represents the complex adjoint of a matrix $M = (m_{i,j})_{i,j=1,\dots,N}$, i.e. $M^* := (\overline{m_{j,i}})_{i,j=1,\dots,N}$, $\overline{M}$ stands for the complex conjugate $\overline{M} := (\overline{m_{i,j}})_{i,j=1,\dots,N}$, and $M^{\mathrm{T}} := (m_{j,i})_{i,j=1,\dots,N}$ is the transposed matrix.

Since $f^{\mathrm{T}} \Sigma K \Sigma^* \overline{f} = \|\mathcal{PT}F\|_{\mathcal{Z}}^2$ is real, Σ is a diagonal matrix, and an inner product has a conjugate symmetry, we can also write

$$\mathcal{R}(F) = \|f\|_{\mathbb{C}^N}^{-2} \cdot \overline{f^{\mathrm{T}} \Sigma K \Sigma^* \overline{f}} = \|f\|_{\mathbb{C}^N}^{-2} \cdot f^* \Sigma^* K^{\mathrm{T}} \Sigma f,$$

where

$$\Sigma^* K^{\mathrm{T}} \Sigma = (\overline{\sigma_m} \, \langle \mathcal{P}v_n, \mathcal{P}v_m \rangle_{\mathcal{Z}} \, \sigma_n)_{m,n=1,\dots,N} \, . \tag{9}$$

[3] The term 'localization' corresponds here to the values τ_n. In typical applications, the norm of $\mathcal{Z}$ will refer to restrictions of functions to a subdomain. In this respect, the obtained functions can be expected to be concentrated to this subdomain (as it is common for Slepian functions). On the other hand, the inverse problem and the decay behaviour of the singular values σ_n also influence the obtained values τ_n.

This result corresponds to the approach for the internal-field-only case in [29].

Example 5.1. We continue with Example 3.3. In this case, the index range is set to $l = 0, \ldots, L$, $m = -l, \ldots, l$. Then the entries of the diagonal matrix Σ are given by

$$\sigma_{l,m} = \left(\frac{r_{\mathrm{p}}}{r_{\mathrm{s}}}\right)^{l}.$$

The unknown vector f contains the Fourier coefficients

$$f_{l,m} = \left\langle F, \frac{1}{r_{\mathrm{p}}} Y_{l,m}\left(\frac{\cdot}{r_{\mathrm{p}}}\right)\right\rangle_{\mathrm{L}^2\left(\Omega_{r_{\mathrm{p}}}\right)}.$$

Furthermore, the matrix K is given by its components

$$\int_R \frac{1}{r_{\mathrm{s}}} Y_{l,m}\left(\frac{\eta}{r_{\mathrm{s}}}\right) \frac{1}{r_{\mathrm{s}}} Y_{l',m'}\left(\frac{\eta}{r_{\mathrm{s}}}\right) \mathrm{d}\omega(\eta).$$

The task is, therefore, to find the eigenvectors f of the matrix

$$\Sigma^* K^{\mathrm{T}} \Sigma = \left[\left(\frac{r_{\mathrm{p}}}{r_{\mathrm{s}}}\right)^{l} \int_R \frac{1}{r_{\mathrm{s}}} Y_{l,m}\left(\frac{\eta}{r_{\mathrm{s}}}\right) \frac{1}{r_{\mathrm{s}}} Y_{l',m'}\left(\frac{\eta}{r_{\mathrm{s}}}\right) \mathrm{d}\omega(\eta) \left(\frac{r_{\mathrm{p}}}{r_{\mathrm{s}}}\right)^{l'}\right]_{\substack{l=0,\ldots,L;\ m=-l,\ldots,l \\ l'=0,\ldots,L;\ m'=-l',\ldots,l'}}.$$

Remark 5.2. For some problems, vectorial (e.g. gradients of potential fields [29]) or tensorial basis functions come into play, and the L^2 inner products involve Euclidean dot products of the kind

$$\langle f, g\rangle_{\mathcal{Z}} = \int_R f(\xi) \cdot g(\xi)\, \mathrm{d}\omega(\xi), \quad f, g \in \mathrm{L}^2\left(R, \mathbb{R}^3\right).$$

In this case, one can make use of this Euclidean product to reduce the numerical expense or the instability of the eigenvalue problem at hand. For example, the vector spherical harmonics (for which we use here the notation in [7]) $y_{l,m}^{(i)}$ can be subdivided into vector fields which are normal to the sphere ($i = 1$) and fields that are tangential to the sphere ($i = 2$ and $i = 3$). For this reason,

$$y_{l,m}^{(1)}(\xi) \cdot y_{n,j}^{(i)}(\xi) = 0$$

holds pointwise (i.e. for all $\xi \in \Omega$) and all $i \in \{2; 3\}$, independently of the degrees l, n and orders m, j. Within the tangential vector fields, such a pointwise, i.e. Euclidean, orthogonality is only obtained for identical degree-order pairs, i.e.

$$y_{l,m}^{(2)}(\xi) \cdot y_{l,m}^{(3)}(\xi) = 0$$

for all $\xi \in \Omega$ and all degrees l and orders m.

In [16], different linear combinations of complex tangential vector spherical harmonics are constructed to obtain alternative basis functions, which we call here $\tilde{y}_{l,m}^{(i)}$, $i = 1, 2, 3$, such that[4]

[4] Note that '$\cdot$' is here the complex dot product, i.e. $w \cdot z := \sum_{j=1}^{3} w_j \overline{z_j}$ for $w, z \in \mathbb{C}^3$.

$$\tilde{y}^{(2)}_{l,m}(\xi) \cdot \tilde{y}^{(3)}_{n,j}(\xi) = 0$$

for all $\xi \in \Omega$, all degrees l, n, and all orders m, j. This pointwise orthogonality can be exploited, because we have

$$\int_R \tilde{y}^{(i_1)}_{l,m}(\xi) \cdot \tilde{y}^{(i_2)}_{n,j}(\xi)\, \mathrm{d}\omega(\xi) = 0$$

whenever $i_1 \neq i_2$. As a consequence, the matrix K can be rearranged into a block matrix

$$\begin{pmatrix} \text{type } i=1 & 0 & 0 \\ 0 & \text{type } i=2 & 0 \\ 0 & 0 & \text{type } i=3 \end{pmatrix}$$

such that the algebraic eigenvalue problems can be solved separately for each type i. This has not only the advantage that the matrices of the eigenvalue problem become smaller (which yields the expectation of a faster and more stable computation of the eigenvectors), it also leads to Slepian functions which are separated by type. This means that the components of the field associated to different types can be independently analyzed by means of Slepian functions.

However, one has to be aware of the fact that the type $i = 2$ of the $y^{(i)}_{l,m}$ (which is a surface gradient field and is, therefore, surface-curl-free) is not the same as the type $i = 2$ of the $\tilde{y}^{(i)}_{l,m}$. The reason is that each tangential $\tilde{y}^{(i)}_{l,m}$, $i \in \{2; 3\}$, is a linear combination of complex versions of $y^{(2)}_{l,m}$ *and* $y^{(3)}_{l,m}$. In particular, $\tilde{y}^{(2)}_{l,m}$ is not surface-curl-free anymore, and $\tilde{y}^{(3)}_{l,m}$ is not surface-divergence-free anymore — properties which the non-tilde versions originally possessed.

For tensor spherical harmonics, there are 9 different types of basis functions, where again some types are orthogonal to each other in the Euclidean sense. Also here, it is possible to define a new basis system such that the Slepian eigenvalue problem can be transformed into 9 independent eigenvalue problems, as shown in [32].

6. Coupled problems

In some applications, we may have data that originate from different causes or sources, and we may be interested in separating them (e.g. internally and externally generated planetary magnetic fields [29]). We will show here that such a scenario can easily be integrated into our general setting.

We now have two operators $\mathcal{T}_1 : \mathcal{X}_1 \to \mathcal{Y}$ and $\mathcal{T}_2 : \mathcal{X}_2 \to \mathcal{Y}$ with svds

$$\mathcal{T}_1 F_1 = \sum_n \sigma^{(1)}_n \left\langle F_1, u^{(1)}_n \right\rangle_{\mathcal{X}_1} v^{(1)}_n, \quad F_1 \in \mathcal{X}_1,$$

$$\mathcal{T}_2 F_2 = \sum_n \sigma^{(2)}_n \left\langle F_2, u^{(2)}_n \right\rangle_{\mathcal{X}_2} v^{(2)}_n, \quad F_2 \in \mathcal{X}_2\,.$$

The notation for the Hilbert spaces and the orthonormal systems is analogous to the previous case. Note that $\mathcal{T}_1$ and $\mathcal{T}_2$ both map into $\mathcal{Y}$, but that they may use different orthonormal systems $(v^{(1)}_n)_n \subset \mathcal{Y}$ and $(v^{(2)}_n)_n \subset \mathcal{Y}$. As in the single-operator case, we have only one Hilbert space $\mathcal{Z}$, one projection $\mathcal{P} : \mathcal{Y} \to \mathcal{Z}$, and one embedding $\iota : \mathcal{Z} \hookrightarrow \mathcal{Y}$.

The inverse problem is now to find $F_1 \in \mathcal{X}_1$ and $F_2 \in \mathcal{X}_2$ such that, for a given $G \in \mathcal{Z}$,

$$\mathcal{P}\mathcal{T}_1 F_1 + \mathcal{P}\mathcal{T}_2 F_2 = G.$$

Example 6.1. In [29], it is assumed that a potential field is given which is a superposition of potentials from an internal and an external source, where the sources could be of a magnetic or a gravitational nature. More precisely, the case of gradients of the potential is considered. For reasons of brevity of the formulae, we will consider here the scalar potential situation. The inner potential corresponds to Example 3.3 and its source is assumed to be located inside the planet (i.e. in the interior of Ω_{r_p}). The external potential originates from a radius of at least r_e, where $r_\mathrm{e} > r_\mathrm{s}$. This leads to the operators

$$\mathcal{T}_1 F_1 = \sum_{l=0}^{\infty} \sum_{m=-l}^{l} \left(\frac{r_\mathrm{p}}{r_\mathrm{s}}\right)^l \left\langle F_1, \frac{1}{r_\mathrm{p}} Y_{l,m}\left(\frac{\cdot}{r_\mathrm{p}}\right)\right\rangle_{\mathrm{L}^2(\Omega_{r_\mathrm{p}})} \frac{1}{r_\mathrm{s}} Y_{l,m}\left(\frac{\cdot}{r_\mathrm{s}}\right), \tag{10a}$$

$$\mathcal{T}_2 F_2 = \sum_{l=0}^{\infty} \sum_{m=-l}^{l} \left(\frac{r_\mathrm{s}}{r_\mathrm{e}}\right)^{l+1} \left\langle F_2, \frac{1}{r_\mathrm{e}} Y_{l,m}\left(\frac{\cdot}{r_\mathrm{e}}\right)\right\rangle_{\mathrm{L}^2(\Omega_{r_\mathrm{e}})} \frac{1}{r_\mathrm{s}} Y_{l,m}\left(\frac{\cdot}{r_\mathrm{s}}\right), \tag{10b}$$

where (10*a*) represents the inner field and (10*b*) stands for the external field. The singular values of $\mathcal{T}_1$ and $\mathcal{T}_2$ both exponentially converge to 0, which means that both operators are compact. However, depending on the values of r_p, r_s, and r_e, these two sequences need not tend to zero equally fast. This means that the associated ill-posednesses need not be equally severe. As a consequence, it can be reasonable to truncate the two series in (10) at different degrees. The consequently different sizes of the orthonormal systems combined with the different instabilities (and, maybe also coupled with different noise scenarios) yield a situation which can be expected to be particularly challenging regarding the necessary regularization.

Let us return to the general setting. For the considered problem, we construct the Hilbert space $\mathcal{X} := \mathcal{X}_1 \otimes \mathcal{X}_2$ as the Cartesian product of the individual spaces, and equip it with the inner product, for $x_1, x_1' \in \mathcal{X}_1$, $x_2, x_2' \in \mathcal{X}_2$,

$$\langle (x_1, x_2), (x_1', x_2') \rangle_{\mathcal{X}} := \langle x_1, x_1' \rangle_{\mathcal{X}_1} + \langle x_2, x_2' \rangle_{\mathcal{X}_2}.$$

Moreover, we define the operator $\mathcal{S} : \mathcal{X} \to \mathcal{Y}$ by

$$\mathcal{S}(F_1, F_2) := \mathcal{T}_1 F_1 + \mathcal{T}_2 F_2, \quad F_1 \in \mathcal{X}_1,\ F_2 \in \mathcal{X}_2\,.$$

Furthermore, we set

$$\begin{aligned} u_{2n} &:= \left(u_n^{(1)}, 0\right), & u_{2n+1} &:= \left(0, u_n^{(2)}\right), \\ v_{2n} &:= v_n^{(1)}, & v_{2n+1} &:= v_n^{(2)}, \\ \sigma_{2n} &:= \sigma_n^{(1)}, & \sigma_{2n+1} &:= \sigma_n^{(2)}. \end{aligned}$$

This arrangement of the two systems into one system certainly does not necessarily have to be done in this order. In particular, in the finite-dimensional case, where we only have $(u_n^{(1)})_{n=1,\ldots,N_1}$ and $(u_n^{(2)})_{n=1,\ldots,N_2}$, we could equivalently set

$$(u_1, \ldots, u_{N_1+N_2}) := \left(u_1^{(1)}, \ldots, u_{N_1}^{(1)}, u_1^{(2)}, \ldots, u_{N_2}^{(2)}\right).$$

We now have

$$\mathcal{S}F = \sum_n \sigma_n \langle F, u_n \rangle_{\mathcal{X}} \, v_n, \quad F \in \mathcal{X},$$

where $(u_n)_n$ is an orthonormal system in $\mathcal{X}$ *but* $(v_n)_n$ is, in general, *not* an orthonormal system in $\mathcal{Y}$. In section 4 we remarked that there is no requirement that $(v_n)_n$ be orthonormal, hence we can proceed now like in the 'non-coupled' case. However, in the (theoretical) case where infinite systems are involved, the particular arrangement of the two systems into one system could be of importance in the sense of the Riemann series theorem (see e.g. [19, p 68])

In the finite-dimensional case, the Slepian matrix,

$$\Sigma^* K^{\mathrm{T}} \Sigma = \left(\overline{\sigma_m} \, \langle \mathcal{P} v_n, \mathcal{P} v_m \rangle_{\mathcal{Z}} \, \sigma_n \right)_{m,n=1,\ldots,N}$$

corresponds to the matrix of the eigenvalue problem for the mixed-source case in [29].

Couplings of more than two sources can be handled analogously.

7. Solving the inverse problem

7.1. The Slepian functions and the svd

The svd for the operator $\mathcal{PT} : \mathcal{X} \to \mathcal{Z}$ in (7), which we know exists, allows us to use a truncated singular-value decomposition

$$F_J = \sum_{\substack{k=1 \\ \tau_k \neq 0}}^{N} \tau_k^{-1} \langle G, h_k \rangle_{\mathcal{Z}} \, g_k \tag{11}$$

as an approximate solution of the inverse problem $\mathcal{PT}F = G$, $G \in \mathcal{Z}$.

To find g_k, h_k, and τ_k, in the finite-dimensional setting of section 5, the procedure requires us to:

- set up the matrix $\Sigma^* K^{\mathrm{T}} \Sigma$ as in (9).
- determine an orthonormal system of eigenvectors[5] $f^{(1)}, \ldots, f^{(N)}$ and its associated eigenvalues $\varrho_1, \ldots, \varrho_N \in \mathbb{R}_0^+$.
- sort the eigenvalues (and the associated eigenvectors) such that $\varrho_1 \geqslant \varrho_2 \geqslant \cdots \geqslant \varrho_N$.
- construct

$$g_k = \sum_{n=1}^{N} f_n^{(k)} u_n \in \mathcal{X}, \quad k = 1, \ldots, N,$$

with the Parseval identity yielding

$$\langle g_k, g_l \rangle_{\mathcal{X}} = \sum_{n=1}^{N} f_n^{(k)} \overline{f_n^{(l)}} = \left\langle f^{(k)}, f^{(l)} \right\rangle_{\mathbb{C}^N} = \delta_{kl}.$$

We now use the g_k as basis functions to expand the solution F, that is, we determine coefficients γ_k such that $F = \sum_{k=1}^{N} \gamma_k g_k$ solves $\mathcal{PT}F = G$. In keeping with the common philosophy of Slepian functions, we may truncate our expansions by taking only these Slepian functions g_k for which $\varrho_k \geqslant \tilde{\varrho}$ for a chosen threshold $\tilde{\varrho}$.

[5] Since $\Sigma^* K^{\mathrm{T}} \Sigma$ is self-adjoint, such an orthonormal basis must exist and all eigenvalues are real. Moreover, since it is a Gramian matrix, all eigenvalues must be non-negative.

In our case, we determine the γ_k from the svd of $\mathcal{PT}$, proceeding as follows. From (4), we know

$$\mathcal{T}g_k = \sum_{n=1}^{N} \sigma_n f_n^{(k)} v_n, \quad k = 1, \ldots, N,$$

and therefore also

$$\mathcal{PT}g_k = \sum_{n=1}^{N} \sigma_n f_n^{(k)} \mathcal{P}v_n, \quad k = 1, \ldots, N.$$

Furthermore, with (9), an interchanging of m and n, and the fact that the $f^{(k)}$ are orthonormal eigenvectors of $\Sigma^* K^{\mathrm{T}} \Sigma$, we get

$$\begin{aligned}
\langle \mathcal{PT}g_k, \mathcal{PT}g_l \rangle_{\mathcal{Z}} &= \sum_{m,n=1}^{N} \sigma_m \overline{\sigma_n} f_m^{(k)} \overline{f_n^{(l)}} \langle \mathcal{P}v_m, \mathcal{P}v_n \rangle_{\mathcal{Z}} \\
&= {f^{(l)}}^* \Sigma^* K^{\mathrm{T}} \Sigma f^{(k)} \\
&= \varrho_k \overline{\langle f^{(l)}, f^{(k)} \rangle_{\mathbb{C}^N}} \\
&= \varrho_k \delta_{k,l}.
\end{aligned}$$

We set

$$\begin{aligned}
h_k &:= \varrho_k^{-1/2} \mathcal{PT}g_k, \quad k = 1, \ldots, N, \quad \text{if } \varrho_k \neq 0, \\
\tau_k &:= \varrho_k^{1/2}, \quad k = 1, \ldots, N, \quad \text{if } \varrho_k \neq 0.
\end{aligned}$$

If $\varrho_k = 0$, then $\mathcal{PT}g_k = 0$ such that we set $\tilde{N} := \max\{k \,|\, \varrho_k \neq 0\}$ and consider $(g_k)_{k=1,\ldots,\tilde{N}}$ as an orthonormal basis of $(\ker \mathcal{PT})^{\perp_{\mathcal{X}}}$, the $\langle \cdot, \cdot \rangle_{\mathcal{X}}$-orthogonal complement of the nullspace of $\mathcal{PT}$.

Then,

$$\mathcal{PT}F = \mathcal{PT} \sum_{k=1}^{\tilde{N}} \langle F, g_k \rangle_{\mathcal{X}} g_k = \sum_{k=1}^{\tilde{N}} \langle F, g_k \rangle_{\mathcal{X}} \tau_k h_k, \quad F \in \operatorname{span}\{g_1, \ldots, g_{\tilde{N}}\}.$$

This is the required svd of $\mathcal{PT} : \mathcal{X} \to \mathcal{Z}$, see (7).

The determination of the truncation parameter J in (11) can be accomplished with any one of the known parameter choice methods for the regularization of inverse problems (see e.g. [12, 46] and the references therein). Furthermore, $(h_k)_{k=1,\ldots,\tilde{N}}$ is an orthonormal system in $\mathcal{Z}$. Moreover, (3) implies that

$$\delta_{kl} = \langle h_k, h_l \rangle_{\mathcal{Z}} = \langle \iota(h_k), \iota(h_l) \rangle_{\mathcal{Y}}$$

such that $(\iota(h_k))_{k=1,\ldots,\tilde{N}}$ is also orthonormal in $\mathcal{Y}$. In our example of function spaces, this means that the $\iota(h_k)$ are spacelimited functions, which are orthogonal in $\mathrm{L}^2(\Omega_{r_s})$.

Example 7.1. We continue with example 5.1, reverting to the degree and order indices $l = 0, \ldots, L$, $m = -l, \ldots, l$. After having obtained the eigenvectors $f^{(k)}$ and eigenvalues ϱ_k for the matrix $\Sigma^* K^{\mathrm{T}} \Sigma$, we can calculate the following functions:

$$g_k(\xi) = \sum_{l=0}^{L} \sum_{m=-l}^{l} f_{l,m}^{(k)} \frac{1}{r_\mathrm{p}} Y_{l,m}\left(\frac{\xi}{r_\mathrm{p}}\right), \quad \xi \in \Omega_{r_\mathrm{p}},$$

$$h_k(\zeta) = \varrho_k^{-1/2} \sum_{l=0}^{L} \sum_{m=-l}^{l} f_{l,m}^{(k)} \left(\frac{r_\mathrm{p}}{r_\mathrm{s}}\right)^l \frac{1}{r_\mathrm{s}} Y_{l,m}\left(\frac{\zeta}{r_\mathrm{s}}\right), \quad \zeta \in R,$$

$$[\iota(h_k)](\eta) = \begin{cases} \varrho_k^{-1/2} \sum_{l=0}^{L} \sum_{m=-l}^{l} f_{l,m}^{(k)} \left(\frac{r_\mathrm{p}}{r_\mathrm{s}}\right)^l \frac{1}{r_\mathrm{s}} Y_{l,m}\left(\frac{\eta}{r_\mathrm{s}}\right), & \eta \in R \\ 0, & \eta \in \Omega_{r_\mathrm{s}} \setminus R \end{cases}, \quad \eta \in \Omega_{r_\mathrm{s}}.$$

We obtain then the following orthogonalities

$$\int_{\Omega_{r_\mathrm{p}}} g_k(\xi)\, g_l(\xi)\, \mathrm{d}\omega(\xi) = \delta_{kl},$$

$$\int_R h_k(\zeta)\, h_l(\zeta)\, \mathrm{d}\omega(\zeta) = \int_{\Omega_{r_\mathrm{s}}} [\iota(h_k)](\eta)\; [\iota(h_l)](\eta)\, \mathrm{d}\omega(\eta) = \delta_{kl}.$$

The example and the considerations above show one of the advantages of Slepian functions applied to inverse problems with regional data. We are able to obtain a singular-value decomposition for the projected operator $\mathcal{PT} : \mathcal{X} \to \mathcal{Z}$, that is, for the case where only regional data are available. We have orthonormal function systems $(g_k)_k$ in $\mathcal{X}$ and $(h_k)_k$ in $\mathcal{Z}$ which can be calculated explicitly.

7.2. Construction of a scaling function as a filter

Moreover, alternative methods like wavelet-based multiscale methods are applicable, where we introduce a filter φ_J, such that

$$\tilde{F}_J = \sum_{k=1}^{\tilde{N}} \varphi_J(k) \tau_k^{-1} \langle G, h_k \rangle_{\mathcal{Z}}\, g_k.$$

In the case of functions, this could be

$$\tilde{F}_J(x) = \langle G, \Phi_J(x, \cdot) \rangle_{\mathcal{Z}},$$

where the scaling function Φ_J is given by

$$\Phi_J(x, z) = \sum_{k=1}^{\tilde{N}} \varphi_J(k)\, \tau_k^{-1}\, \overline{g_k(x)}\, h_k(z). \tag{12}$$

We will further elaborate this in section 8.

7.3. Infinite-dimensional case

Putting numerical considerations aside for a moment, we can observe that the considerations here are not restricted to the finite-dimensional case. With the (initially unknown but definitely existing) singular-value decomposition (7) and with (8), we could also proceed with an infinite (e.g. non-bandlimited) setting. We would get a (possibly infinite, but countable) system of non-negative values $(\tau_k)_{k\in\kappa} = (\varrho_k^{1/2})_{k\in\kappa}$, where $\kappa \subset \mathbb{N}$ stands here for the index

range which counts all such singular values. Due to the nature of an svd, the g_k, $k \in \kappa$, would represent an orthonormal system in $\mathcal{X}$. More precisely, we would have an orthonormal basis of $(\ker \mathcal{PT})^{\perp_{\mathcal{X}}}$. Then

$$h_k = \tau_k^{-1} \mathcal{PT} g_k, \quad k \in \kappa,$$

is an orthonormal system such that $\operatorname{im} \mathcal{PT} \subset \overline{\operatorname{span}\{h_k \mid k \in \kappa\}}^{\|\cdot\|_{\mathcal{Z}}}$ (the closure of the span of h_k, i.e. every element in the image of $\mathcal{PT}$ can be expanded into the basis h_k, possibly with an infinite number of summands). Furthermore, we would also get that $(\iota(h_k))_{k\in\kappa}$ is orthonormal in $\mathcal{Y}$ due to ι being an isometry.

8. Scaling functions, wavelets, reproducing kernels and Fredholm integral operators

In this section, we assume that the Hilbert spaces $\mathcal{X}$, $\mathcal{Y}$, and $\mathcal{Z}$ are spaces of functions with domains X, Y, and Z, respectively. The example of downward continuation which has been discussed throughout this paper fits this assumption.

For an $F \in \mathcal{X}$, a $G \in \mathcal{Z}$, we use the svd of the problem $\mathcal{PT}F = G$,

$$\begin{aligned}(\mathcal{PT}F)(z) &= \sum_{k\in\kappa} \tau_k \langle F, g_k\rangle_{\mathcal{X}}\, h_k(z)\\ &= \left\langle F(\cdot), \sum_{k\in\kappa} \tau_k\, g_k(\cdot)\, \overline{h_k(z)} \right\rangle_{\mathcal{X}}\\ &= \left\langle F(\cdot), D^{\uparrow}(z,\cdot)\right\rangle_{\mathcal{X}},\end{aligned}$$

to define now the following functions

$$\begin{aligned}D^{\uparrow}(z,x) &:= \sum_{k\in\kappa} \tau_k\, \overline{h_k(z)}\, g_k(x), \quad z \in Z,\ x \in X,\\ D^{\downarrow}(x,z) &:= \sum_{k\in\kappa} \tau_k^{-1}\, \overline{g_k(x)}\, h_k(z), \quad x \in X,\ z \in Z,\end{aligned}$$

assuming appropriate convergence[6] in the case of an infinite number of summands. Similarly,

$$\begin{aligned}\left([\mathcal{PT}]^{+}G\right)(x) &= \sum_{k\in\kappa} \tau_k^{-1} \langle G, h_k\rangle_{\mathcal{Z}}\, g_k(x)\\ &= \left\langle G(\cdot), \sum_{k\in\kappa} \tau_k^{-1}\, h_k(\cdot)\, \overline{g_k(x)} \right\rangle_{\mathcal{Z}}\\ &= \left\langle G(\cdot), D^{\downarrow}(x,\cdot)\right\rangle_{\mathcal{Z}}, \quad x \in X,\end{aligned}$$

where $(\mathcal{PT})^{+} = (\mathcal{PT}|_{(\ker(\mathcal{PT}))^{\perp_{\mathcal{X}}}})^{-1}$ is the Moore-Penrose inverse of $\mathcal{PT}$.

The kernel $D^{\downarrow}$ probably will not exist in the infinite-dimensional case, because (τ_k^{-1}) diverges to $+\infty$. This represents the ill-posedness of the problem, because $(\mathcal{PT})^{+}G$ cannot so easily be computed. For this reason, a regularization is needed.

This can be done in manifold ways, where a truncation of the series, which would be the classical Slepian function approach discussed above in (11), is one out of these possibilities.

[6] We need that, for each fixed $z \in Z$, the series corresponding to $D^{\uparrow}(z,\cdot)$ converges strongly in the sense of $\|\cdot\|_{\mathcal{X}}$. Analogously, for each fixed $x \in \mathcal{X}$, the series corresponding to $D^{\downarrow}(x,\cdot)$ must be strongly convergent in the sense of $\|\cdot\|_{\mathcal{Z}}$.

The more general Ansatz corresponds to the scaling function approach described above in (12), where we replace $D^{\downarrow}$ by the kernel

$$\Phi_J(x,z) = \sum_{k\in\kappa} \varphi_J(k)\,\tau_k^{-1}\,\overline{g_k(x)}\,h_k(z), \quad x \in X,\, z \in Z.$$

By choosing a sequence $(\varphi_J(k))_k$, which tends to zero 'sufficiently' fast, we can control the rising inverse singular values τ_k^{-1} and obtain a stable solution. Such wavelet-based regularization methods have already been discussed for such general Hilbert space settings in [8, 23]. We will show here the most important properties of such a multiscale regularization for the considered Slepian-function approach.

Theorem 8.1. *Let the assumptions from above hold true. Moreover, let the family of functions $\varphi_J : \mathbb{R}_0^+ \to \mathbb{R}_0^+$, $J \in \mathbb{N}_0$, satisfy the following conditions*[7]*:*

(i) for all $J \in \mathbb{N}_0$ and all $x \in X$, the following series converges pointwise:

$$\sum_{k\in\kappa} \left|\varphi_J(k)\,\overline{g_k(x)}\,\tau_k^{-1}\right|^2 < +\infty, \tag{13}$$

(ii) for all $J \in \mathbb{N}_0$,

$$\sup_{k\in\kappa} \left(\varphi_J(k)\tau_k^{-1}\right) < +\infty, \tag{14}$$

(iii) for all $k \in \kappa$,

$$\lim_{J\to\infty} \varphi_J(k) = 1, \tag{15}$$

(iv) for all $J \in \mathbb{N}_0$ and all $k \in \kappa$,

$$0 \leqslant \varphi_J(k) \leqslant 1. \tag{16}$$

Furthermore, the sequence of functions $\Phi_J * G \in \mathcal{X}$, $J \in \mathbb{N}_0$, is defined by

$$(\Phi_J * G)(x) := \left\langle G(\cdot), \sum_{k\in\kappa} \varphi(k)\,\tau_k^{-1}\,\overline{g_k(x)}\,h_k(\cdot)\right\rangle_{\mathcal{Z}}, \quad x \in X,\, G \in \mathcal{Z}. \tag{17}$$

Then

$$\lim_{J\to\infty} \left\|[\mathcal{P}\mathcal{T}]^+ G - \Phi_J * G\right\|_{\mathcal{X}} = 0$$

for all $G \in \mathrm{im}(\mathcal{P}\mathcal{T})$. Moreover, each mapping

$$\begin{aligned} &\mathcal{Z} \to \mathcal{X} \\ &G \mapsto \Phi_J * G, \end{aligned}$$

$J \in \mathbb{N}_0$, is continuous.

Before we prove this theorem, let us state what it means for the inverse problem. The sequence $(\Phi_J * G)_J$ converges strongly (in the $\|\cdot\|_{\mathcal{X}}$-sense) to the solution $F \in (\ker(\mathcal{P}\mathcal{T}))^{\perp_{\mathcal{X}}}$ of the inverse problem $\mathcal{P}\mathcal{T}F = G$, provided that a solution exists (i.e. $G \in \mathrm{im}(\mathcal{P}\mathcal{T})$). Hence, we can construct approximate solutions which are arbitrarily close to the exact solution.

[7] If κ is a finite set, then conditions (i) and (ii) are trivially satisfied.

However, in contrast to the exact solution F, which discontinuously depends on G in the infinite-dimensional case (remember that $\mathcal{PT}$ is compact), the approximations are stable, that is they continuously depend on the data G. This also yields the expectation of numerically stable approximate inversions in the finite-dimensional case.

Let us now prove the theorem.

Proof. From the condition in (13), we obtain that the series

$$\sum_{k\in\kappa} \varphi_J(k)\,\tau_k^{-1}\,\overline{g_k(x)}\,h_k(\cdot),$$

with arbitrary but fixed $J \in \mathbb{N}$ and $x \in X$, converges strongly in $\mathcal{Z}$. Hence, we are allowed to interchange the inner product with the series in (17) and get

$$(\Phi_J * G)(x) = \sum_{k\in\kappa} \varphi_J(k)\,\tau_k^{-1}\,\langle G, h_k\rangle_{\mathcal{Z}}\,g_k(x)$$

for all $J \in \mathbb{N}_0$ and all $x \in X$. Furthermore, the solvability of the inverse problem $\mathcal{PT}F = G$ yields a unique (minimum-norm) solution $F \in (\ker(\mathcal{PT}))^{\perp_{\mathcal{X}}}$, which is given by

$$F = \sum_{k\in\kappa} \tau_k^{-1}\,\langle G, h_k\rangle_{\mathcal{Z}}\,g_k$$

in the sense of $\|\cdot\|_{\mathcal{X}}$. Hence, the well-known Picard condition

$$\sum_{k\in\kappa} \left|\tau_k^{-1}\,\langle G, h_k\rangle_{\mathcal{Z}}\right|^2 < +\infty$$

must hold. This Picard condition in combination with (16) implies that the series

$$\|F - \Phi_J * G\|_{\mathcal{X}}^2 = \sum_{k\in\kappa} \left|(1-\varphi_J(k))\,\tau_k^{-1}\,\langle G, h_k\rangle_{\mathcal{Z}}\right|^2$$

uniformly converges with respect to all $J \in \mathbb{N}$. Hence,

$$\begin{aligned}\lim_{J\to\infty} \|F - \Phi_J * G\|_{\mathcal{X}}^2 &= \lim_{J\to\infty} \sum_{k\in\kappa} \left|(1-\varphi_J(k))\,\tau_k^{-1}\,\langle G, h_k\rangle_{\mathcal{Z}}\right|^2 \\ &= \sum_{k\in\kappa} \left|\left(1 - \lim_{J\to\infty}\varphi_J(k)\right)\tau_k^{-1}\,\langle G, h_k\rangle_{\mathcal{Z}}\right|^2 \\ &= 0\end{aligned}$$

due to (15).

For proving the stability of the approximations $\Phi_J * G$, we have a look at

$$\begin{aligned}\|\Phi_J * G\|_{\mathcal{X}}^2 &= \sum_{k\in\kappa} \left|\varphi_J(k)\,\tau_k^{-1}\,\langle G, h_k\rangle_{\mathcal{Z}}\right|^2 \\ &\leqslant \sup_{k\in\kappa} \left(\varphi_J(k)\,\tau_k^{-1}\right)^2 \sum_{k\in\kappa} |\langle G, h_k\rangle_{\mathcal{Z}}|^2 \\ &= \sup_{k\in\kappa} \left(\varphi_J(k)\,\tau_k^{-1}\right)^2 \|G\|_{\mathcal{Z}}^2, \quad G \in \mathcal{Z}. \end{aligned} \tag{18}$$

According to (14), the supremum in (18) is finite. This proves the continuity of the mapping. □

Examples for the choice of φ_J can be constructed out of generators of scaling functions as they are known, for instance, from the theory of spherical wavelets (see e.g. [7, sections 11.3 and 11.4, [23, example 2.3.7], and [25, example 7.20]). However, the critical part is represented by conditions (i) and (ii). They can be trivially satisfied by taking generators of bandlimited scaling functions, that is functions φ_J with compact support $\operatorname{supp}\varphi_J$ for each $J \in \mathbb{N}_0$. In the non-bandlimited case, where the support is unbounded for an infinite number of scales J, the particular properties of the computed Slepian functions g_k and the rate of divergence of the inverse singular values (τ_k^{-1}) have to be taken into account. On the one hand, this yields an interesting challenge for future research, because these requirements implicitly also include the geometry of the region R (as well as the degree of the ill-posedness of the original inverse problem $\mathcal{T}F = G$) into the conditions on φ_J. On the other hand, in practice, one either always has to restrict the calculations to finite dimensional spaces, that is, to the bandlimited case, or κ is a finite set to begin with.

In this context, the influence of the geometry and size of the region on the one hand and the ill-posedness of the (original, unrestricted) inverse problem on the other hand on the singular values (τ_k) should be further investigated. Moreover, it should be noted that, by choosing only a finite number of Slepian functions (which is, so far, the only numerically feasible way), a regularization is already included. Indeed, it appears to be reasonable to discuss the parameter choices concerning the selection of the φ_J and the size of the Slepian basis together as one regularization method. The details of the practical implementation and the underlying theory shall be addressed in a future research project of the authors.

Note also that, in the particular case of L^2-inner products in $\mathcal{X}$ and $\mathcal{Z}$, we can, indeed, write the inverse problem as a Fredholm integral equation of the first kind

$$(\mathcal{P}\mathcal{T}F)(z) = \int_X F(x)\,\overline{D^{\uparrow}(z,x)}\,\mathrm{d}x, \quad z \in Z.$$

Let us discuss now a special case: $\mathcal{T} = \mathcal{I}$ (identity) and $\mathcal{X} = \mathcal{Y}$, i.e. we 'simply' want to interpolate/approximate a function. In this case, $u_n = v_n$ for all n and $\sigma_n = 1$ for all n. The singular-value decomposition of $\mathcal{T}$ would be representable as

$$\mathcal{T}F = \sum_n \langle F, u_n\rangle_{\mathcal{X}}\, u_n, \quad F \in \mathcal{X}.$$

The task is still to find a new singular-value decomposition for the projected equation, but this time it is only the projection itself which needs the svd. We, therefore, look for a representation of the form

$$\mathcal{P}F = \sum_k \tau_k \langle F, g_k\rangle_{\mathcal{X}}\, h_k$$

which originates in the same way from the eigenvalue- or singular-value-problem discussed above, where now $h_k = \varrho_k^{-1/2}\mathcal{P}g_k = \tau_k^{-1}\mathcal{P}g_k$. If $\mathcal{P}$ is the restriction operator $\mathcal{P} : F \mapsto F|_Z$, then

$$D^{\uparrow}(z,x) = \sum_{k\in\kappa} \overline{g_k(z)}\, g_k(x), \quad z \in Z,\ x \in X,$$

$$D^{\downarrow}(x,z) = \sum_{k\in\kappa} \tau_k^{-2}\, \overline{g_k(x)}\, g_k(z), \quad x \in X,\ z \in Z.$$

In other words, using again L^2-inner products, we see that

$$\int_X F(x)\overline{D^{\uparrow}(z,x)}\,\mathrm{d}x = (\mathcal{P}F)(z) = F(z), \quad z \in Z,$$

reproduces F on the subset $Z \subset Y = X$. In particular,

$$\int_X g_k(x)\overline{D^{\uparrow}(z,x)}\,\mathrm{d}x = (\mathcal{P}g_k)(z) = g_k(z), \quad z \in Z.$$

Vice versa,

$$\int_Z F(z)\overline{D^{\downarrow}(x,z)}\,\mathrm{d}z = \left(\mathcal{P}^{+}F\right)(x), \quad x \in X,$$

reconstructs F on the whole set X from knowledge of F on the subset Z. The latter sounds confusing at the first sight. How could the continuation of F to a larger set be unique? Indeed, there is a catch: the series of $D^{\downarrow}$ must converge. This can be satisfied in two cases:

- either κ is finite: then the function spaces under investigation have finite dimensions and the functions in it are, indeed, uniquely determined by their values on a subset (like it is e.g. the case for polynomials up to a fixed degree),
- or κ is infinite but the series converges nevertheless: then this implies certain restrictions on the functions in the space for which $D^{\downarrow}$ is a reproducing kernel. For example, an ill-posed problem where $(\tau_k^{-1})_k$ is unbounded would require the sequence $(g_k)_k$ to rapidly decay such that $D^{\downarrow}$ exists. If we assume that large values of k could refer to a higher oscillatory behaviour (this is well-known for orthogonal polynomials and numerical experiences show that some Slepian functions also have this property), then the required decay with respect to k also has an influence on the functions F to which the reproducing kernel is applicable and which have to be spanned by the g_k.

Note that experience with Slepian functions shows that the eigenvalues often separate into a set of values close to 1 and some others which are almost 0. This also demonstrates the difficulty of finding a numerically stable kernel $D^{\downarrow}$, since then some τ_k^{-2} are very large.

Remark 8.2. Since the scaling functions Φ_J provide us with different approximations $\Phi_J * F$ to F, it also appears to be useful to look at differences $\Psi_J := \Phi_{J+1} - \Phi_J$ such that

$$\Phi_{J+1} * G = \Phi_J * G + \Psi_J * G.$$

Here, $\Psi_J * G$ can be regarded as the detail information which is added to the approximation $\Phi_J * G$ at scale J to obtain the approximation $\Phi_{J+1} * G$ at the next scale. In analogy to common wavelet theories, where such scale-step properties also exist, the kernels Ψ_J can be called wavelets here.

9. Some numerical tests

This paper generalizes an approach presented in [29] for the downward continuation of geophysically relevant potentials. Their application has served as a thread in this paper to show that the general setup, indeed, includes this particular example. Rather than experimenting with the same examples again, we demonstrate the applicability of the general Ansatz to other inverse problems by discussing some enlightening problems on the 1-sphere. All numerical calculations were done with `MatlabR2015b`.

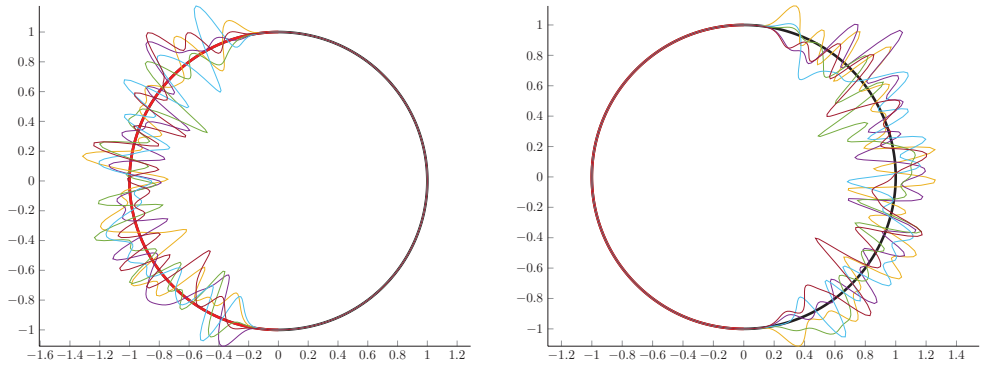

Figure 1. Eigenfunctions $g_1, \ldots, g_6$ (left) corresponding to the largest eigenvalues and $g_{96}, \ldots, g_{101}$ (right) corresponding to the smallest eigenvalues, the subdomain R is shown in red; note that each Slepian function was multiplied with the same factor to scale the amplitudes for better visibility.

9.1. Identity

We start with an approximation problem. The Hilbert spaces and the operator (which is the identity operator for an approximation problem) are chosen as follows:

$$\mathcal{X} := \mathrm{L}^2[0, 2\pi], \qquad \mathcal{Y} := \mathcal{X}, \qquad \mathcal{Z} := \mathrm{L}^2\left[\frac{\pi}{2}, \frac{3\pi}{2}\right],$$
$$T := \mathrm{Id}, \qquad \sigma_n := 1 \quad \text{for all } n.$$

Note that $\mathrm{L}^2[0, 2\pi]$ is isometric and isomorphic to $\mathrm{L}^2(\mathbb{S}^1)$, where $\mathbb{S}^1$ is the 1-sphere.

Moreover, we need orthonormal basis systems for the Hilbert spaces involved. We take here a common system, for $x \in [0, 2\pi]$,

$$u_{0,1}(x) := \frac{1}{\sqrt{2\pi}},$$
$$u_{n,1}(x) := \frac{1}{\sqrt{\pi}} \cos(nx), \qquad u_{n,2}(x) := \frac{1}{\sqrt{\pi}} \sin(nx), \quad n \geqslant 1,$$
$$v_{n,j}(x) := u_{n,j}(x) \quad \text{for all } n, j.$$

For calculating the Slepian functions, the bandlimit is set to $N := 50$. Moreover, we use the transformation

$$k(n, j) = \begin{cases} 2(n-1) + j + 1, & \text{if } n \geqslant 1 \\ 1, & \text{if } n = 0 \end{cases}$$

to have a single index only. A selection of the Slepian functions on the 1-sphere $\mathbb{S}^1$ with largest and lowest eigenvalues is shown in figure 1. It can be seen that the set of Slepian functions can be subdivided into functions with a strong localization in $R = [0.5\pi, 1.5\pi]$ and other functions which concentrate on the complement $D \setminus R = [0, 0.5\pi[\cup]1.5\pi, 2\pi]$. This is also confirmed by the eigenvalues, which are shown in figure 2. For numerical reasons, we only consider Slepian functions for which $\tau_k \geqslant 0.1\% \cdot \tau_1$ in all our calculations.

The Fourier coefficients of the contrived solution F are chosen by

$$\langle F, u_k \rangle_{\mathcal{X}} := (1 + \varepsilon_k) \frac{1}{k}, \quad k = 1, \ldots, 2N + 1.$$

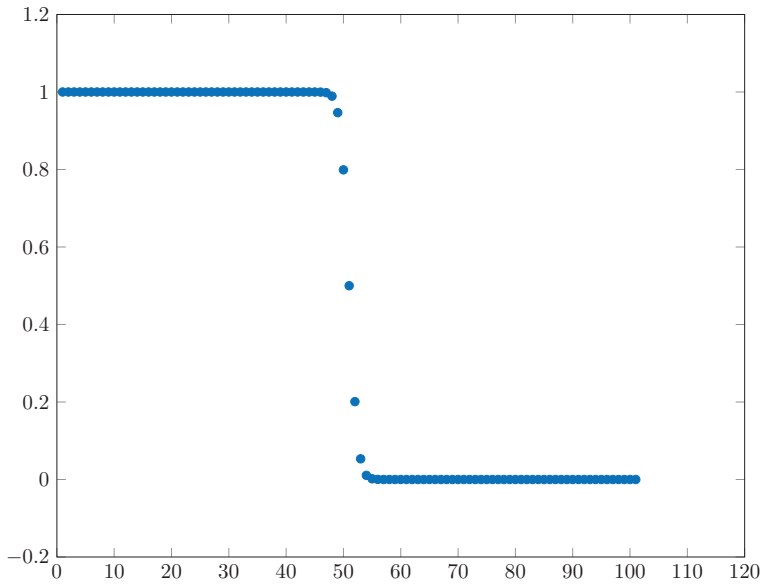

Figure 2. Eigenvalues (sorted) for the Slepian localization problem: there is a sharp transition from strong to weak localization.

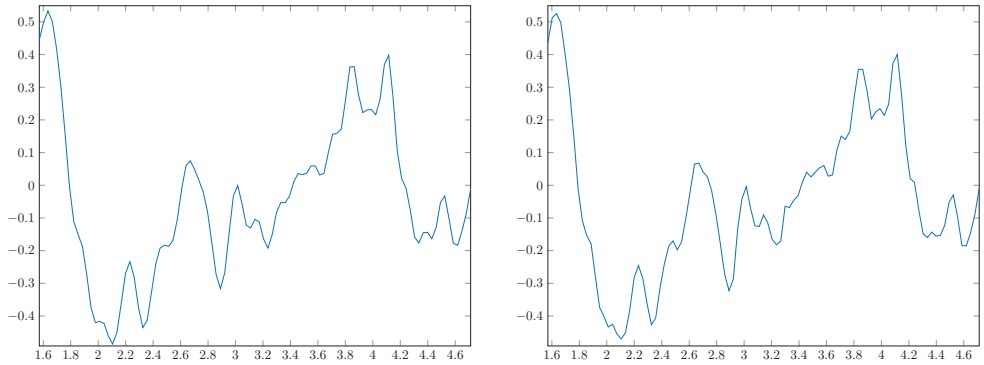

Figure 3. Right-hand side G for the approximation problem without noise (left) and after adding the noise (right).

The ε_k are standard normally distributed random numbers. The corresponding function is represented by the red graphs in figures 4 and 5. The right-hand side is calculated as $G = \mathcal{P}\mathcal{T}F = F|_{[0.5\pi,1.5\pi]}$ on an equidistant grid of 1001 points in $[0.5\pi, 1.5\pi]$. This right-hand side is contaminated with noise by replacing G with $G + 0.01\,\tilde{\varepsilon}_k$ (see figure 3), where the $\tilde{\varepsilon}_k$ are standard normally distributed random variables (ε_k and $\tilde{\varepsilon}_k$ were obtained with the `MATLAB` function `randn`). Moreover, the functions φ_J are chosen as the generators of the Shannon scaling function (see e.g. [7]) such that

$$\varphi_J(k) = \begin{cases} 1, & \text{if } k < 2^J \\ 0, & \text{else} \end{cases}, \quad J, k \in \mathbb{N}_0.$$

For the convolution $\langle \Phi_J(x,\cdot), G\rangle_{\mathcal{Z}}$, a composite Simpson's rule was used. The points x_i used for plotting $\langle \Phi_J(x,\cdot), G\rangle_{\mathcal{Z}}$ are on an equidistant grid of 401 points in $[0, 2\pi]$.

Table 1. Errors (rms) for the pure approximation problem depending on the scale J for the Shannon scaling function Φ_J.

Scale	Error
1	0.238 46
2	0.235 66
3	0.218 51
4	0.183 88
5	0.121 27
6	0.002 4189
7	0.002 4189

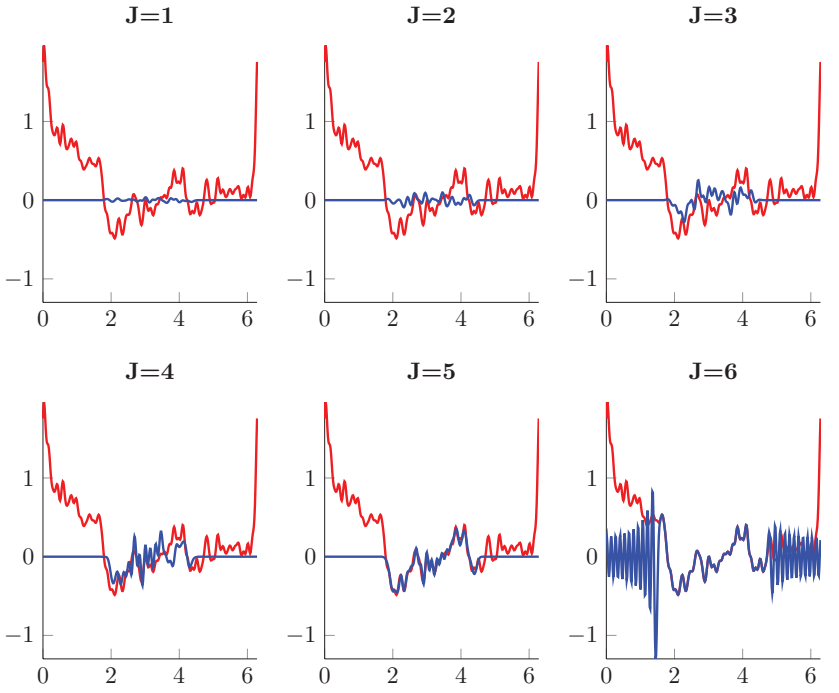

Figure 4. Solution (red) and multi-scale approximations (blue) at different scales J, shown on the whole domain D: at a sufficiently large scale, we obtain a very good approximation to the projection $\mathcal{P}F$ of F to the subinterval R.

The root mean square error $(\frac{1}{M}\sum_{i=1}^{M}(F(x_i)-(\Phi_J * G)(x_i))^2)^{1/2}$ is calculated only for points x_i in $R=[0.5\pi, 1.5\pi]$ and is shown in table 1. The approximation error clearly decreases and then stagnates at a low level (note that the truncation condition $\tau_k < 0.1\% \cdot \tau_1$ is achieved in this example for $k=60$; hence, we have here that $\varphi_{J_1}(k)=\varphi_{J_2}(k)$ for all $k=1,\ldots,101$, if $J_1, J_2 \geqslant 6$). Note that the values of F vary within R between -0.5 and 0.5. The obtained approximations are shown in figures 4 and 5. We can see that the chosen function F is well approximated on the interval R. For the larger scale $J=6$, some boundary effects[8] occur,

[8] We experienced in our experiments that a finer quadrature grid of 10,001 points for the Simpson rule reduces these effects in their amplitude such that they can partially also occur due to inaccuracies in the numerical integration; however, also with this finer grid, the effects were still clearly visible. This is due to the fact that the scaling function of scale $J=6$ also contains some functions g_k which are not well-localized, see figure 2.

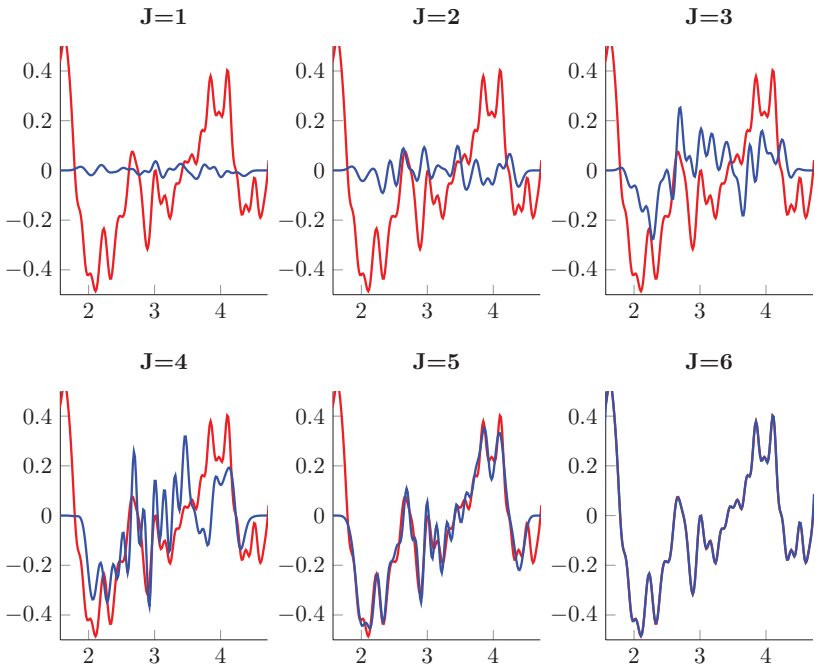

Figure 5. Solution (red) and multi-scale approximations (blue) at different scales J, shown on the subdomain R: at scale $J = 6$, the projection $\mathcal{P}F$ can hardly be distinguished from the approximation $\Phi_J * G$.

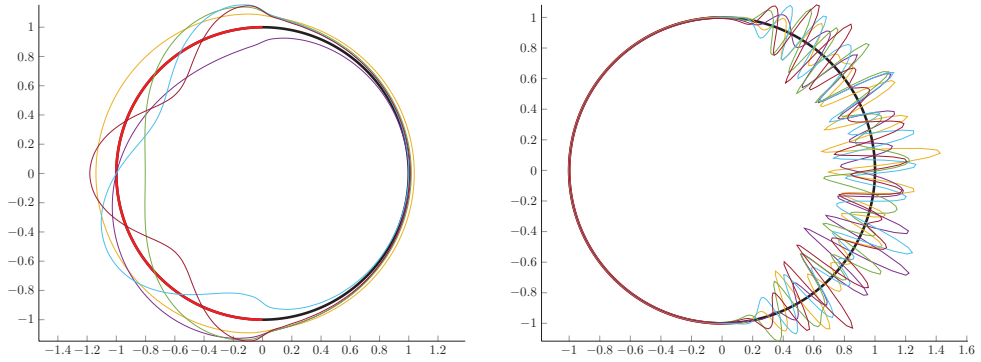

Figure 6. Eigenfunctions $g_1, \ldots, g_6$ (left) and $g_{96}, \ldots, g_{101}$ (right) for the case of the chosen inverse problem, the subdomain R is shown in red; note that each Slepian function was multiplied with the same factor to scale the amplitudes for better visibility.

which shows that, in some cases, smoother approximations at lower scales (like here for $J = 5$), which are still close to the exact solution but do not show such boundary effects, might be preferred.

9.2. An inverse problem

We now consider an ill-posed inverse problem. The spaces $\mathcal{X}$, $\mathcal{Y}$, and $\mathcal{Z}$ as well as their orthonormal basis systems are chosen like above. However, the singular values are now given by

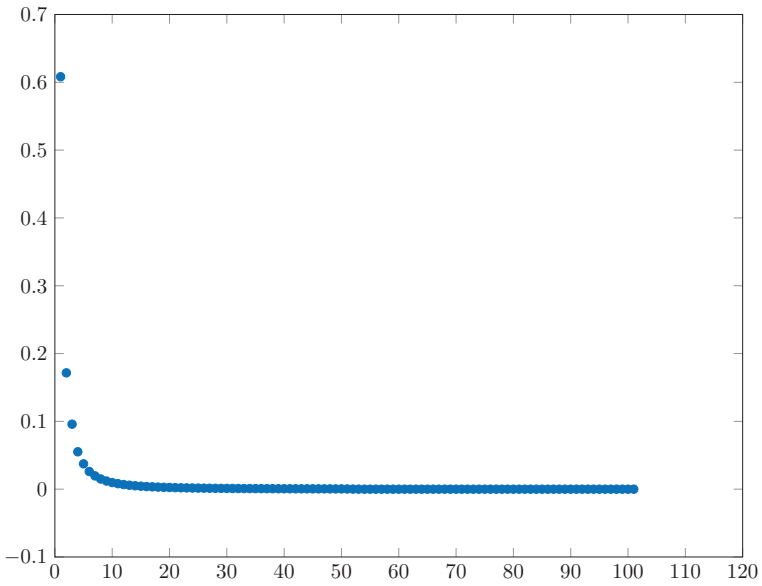

Figure 7. Eigenvalues (sorted) for the Slepian localization problem and the case of the chosen inverse problem: the ill-posedness is also reflected in the eigenvalues.

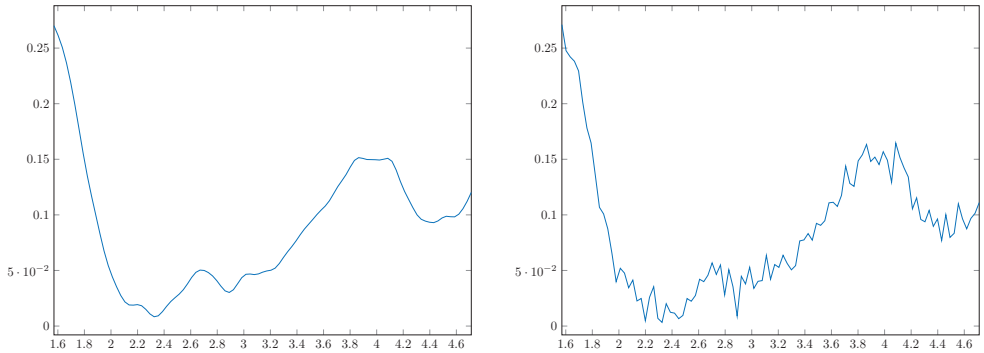

Figure 8. Right-hand side G for the inverse problem without noise (left) and after adding the noise (right): due to the decreasing singular values, the amplitude of G is smaller than the amplitude of F such that the noise has a stronger influence than in the approximation problem above.

$$\sigma_{n,j} = \frac{1}{n+1} \quad \text{for all } n, j.$$

In figures 6 and 7, we can see that the Slepian functions and their eigenvalues are indeed influenced by the ill-posed nature of the problem.

Again, the bandlimit is set to $N := 50$. We also take the same function F as the solution of $\mathcal{P}\mathcal{T}F = G$. The right-hand side G is shown in figure 8.

The rest of the numerical calculations is performed like above. The results are shown in table 2 and figures 9 and 10 (here, the truncation condition $\tau_k < 0.1\% \cdot \tau_1$ is reached for $k = 58$ such that the approximations again stagnate from scale $J = 6$). Clearly, the noise has

Table 2. Errors (rms) depending on the scale for the Shannon scaling function for the inverse problem.

Scale	Error
1	0.305 31
2	0.327 36
3	0.281 18
4	0.279 93
5	0.288 08
6	0.167 88
7	0.167 88

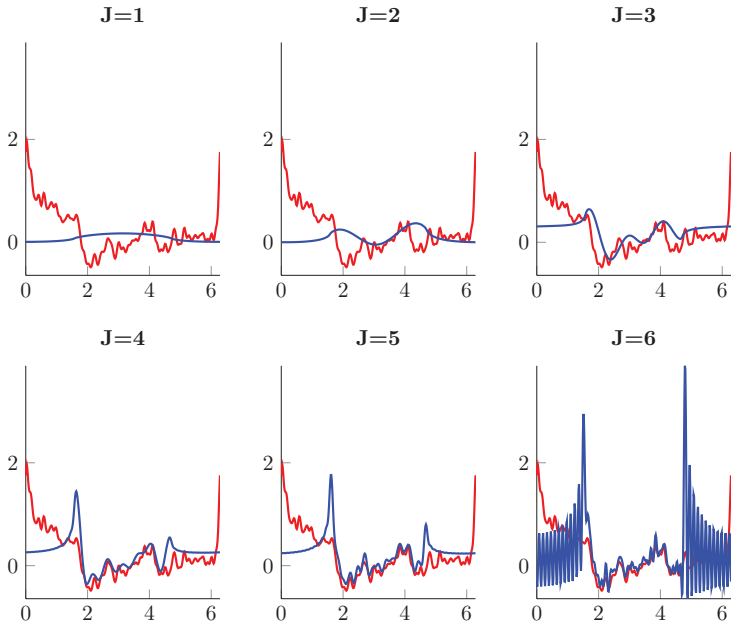

Figure 9. Solution of the inverse problem (red) and multi-scale approximations (blue) at different scales J, shown on the whole domain D: in view of the ill-posed nature of the problem, the approximations are still rather close to the solution F on the subdomain R.

much more influence on the solution of the ill-posed problem. However, the approximations at sufficiently large scales are still rather close to the exact (noise-free) solution.

We can also see that the multiscale approach is appropriate for smoothing the solution. For example, scales $J = 3$ and $J = 4$ reveal trends in the solution which are smooth and coarse (i.e. associated to a low frequency). This is, for example, useful, if a very noisy signal can be expected or if one is interested in separating the phenomena of different 'wavelengths' (in a more abstract sense) in the solution.

In figures 11 and 12, we show some scaling functions $\Phi_J(x, \cdot)$ and wavelets $\Psi_J(x, \cdot)$, respectively, for different fixed points x (one inside the region R and one outside) and different scales. One can see two effects: first, for larger scales, the scaling functions get larger values. Second, for points x away from the region R, the scaling functions are much smaller in the amplitude, because they are built of Slepian functions with a good localization in R.

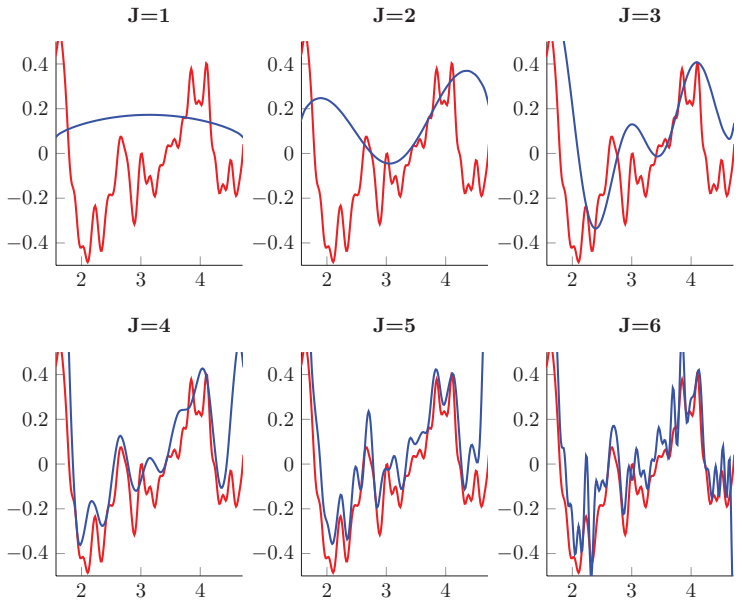

Figure 10. Solution of the inverse problem (red) and multi-scale approximations (blue) at different scales J, shown on the subdomain R: the approximations are relatively close to the exact solution. Depending on the scale, the approximations are more or less filtered as the varying smoothness shows.

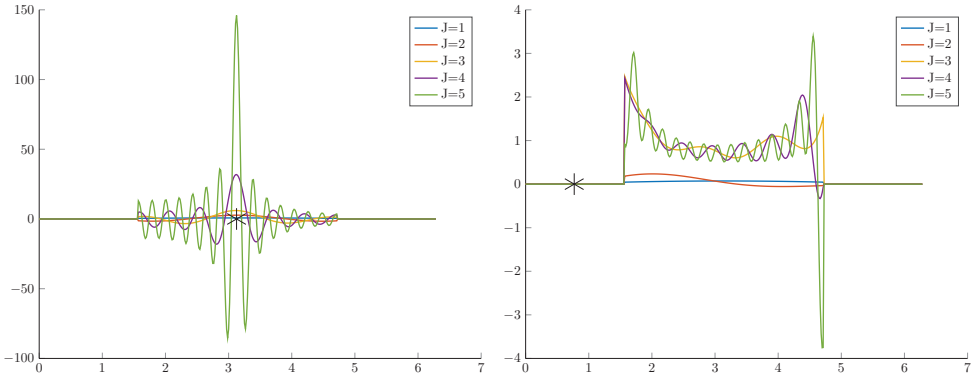

Figure 11. Scaling functions $\Phi_J(x,\cdot)$ for different scales and points x (asterisk) approximately in the centre of R (left) and away from R (right).

The wavelets show similar properties accordingly. Moreover, the kernels Φ_J and Ψ_J not only inherit the concentration to the region R from the Slepian functions. The increasing oscillatory behaviour of Slepian functions, which is often observed, also yields that scaling functions and wavelets of larger scales are more oscillatory and can, thus, also reproduce low-wavelength effects in the investigated signal.

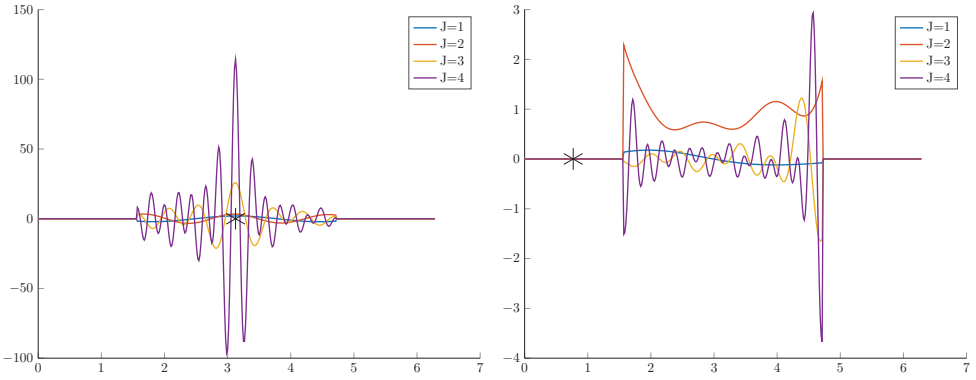

Figure 12. Wavelets $\Psi_J(x,\cdot)$ for different scales and points x (asterisk) approximately in the centre of R (left) and away from R (right).

10. Conclusions

We presented a method for the regularization of linear ill-posed problems as they arise in the geosciences and numerous other disciplines, where the data are only regionally given, and where the singular-value decomposition (svd) of the corresponding compact operator $\mathcal{T}$ needs to be known only for the global case. To treat the case of regional data, we introduced a projection operator $\mathcal{P}$, which could be the restriction of functions on the global domain $\tilde{D}$ to a regional subdomain R. The idea of the methodology is based on the interpretation of the quotient of the norm of the range of $\mathcal{PT}$ and the norm of the preimage as analogous to the energy ratio as used for the construction of Slepian functions. The supremum of this quotient is also the operator norm of $\mathcal{PT}$. Orthonormal 'Slepian' basis functions are found for the preimage which eventually leads to the calculation of an svd of the restricted operator $\mathcal{PT}$. This also provides us with basis functions which are orthogonal in the image spaces of $\mathcal{PT}$ as well as $\mathcal{T}$. The singular values of $\mathcal{PT}$ are linked to the maximized norm quotient, and are diagnostic of the numerical stability and ill-posedness of the inverse problem. We presented an algorithm for determining the Slepian functions and the corresponding svd. We showed how a wavelet multi-scale regularization can be constructed for a variety of different filter functions. Two numerical examples yielded promising results. Our paper is an abstract generalization and an illumination of the fundamental mathematical principles underlying the method introduced in [29]. In particular, we show how complicated problems with coupled sources can be integrated into our conceptual framework.

Practical examples where data are only regionally available or where the analysis is only of interest in a particular subdomain are abundant. In addition, we are often confronted with the situation that the function of interest cannot be measured directly but is only available via the solution of an ill-posed inverse problem. The combination of both challenges (regional analysis and ill-posed inverse problem) occurs rather often. We are now in the position to further investigate the various possibilities that Slepian functions provide for such inverse problems.

Acknowledgments

VM is grateful for the kind hospitality of Princeton University and, in particular, of his host FJS during VM's sabbatical. The discussions during our joint time at Princeton motivated this paper. This work was partially supported by the Deutsche Forschungsgemeinschaft via grants MI 655/7-2 and MI 655/10-1 to VM, and by the US National Aeronautics and Space

Administration via grant NNX14AM29G to FJS and Alain Plattner, and by the US National Science Foundation via grant EAR-1550389 to FJS and Alain Plattner. The authors also wish to thank the anonymous referees for their valuable suggestions.

ORCID iDs

Volker Michel https://orcid.org/0000-0002-2551-0491
Frederik J Simons https://orcid.org/0000-0003-2021-6645

References

[1] Abdelmoula A, Moakher M and Philippe B 2015 A Slepian framework for the inverse problem of equivalent gravitational potential generated by discrete point masses *Inverse Problems Sci. Eng.* **23** 331–50
[2] Albertella A, Sansò F and Sneeuw N 1999 Band-limited functions on a bounded spherical domain: the Slepian problem on the sphere *J. Geodesy* **73** 436–47
[3] Belikov M V and Groten E 1993 Pseudo-harmonic analysis of gravity gradients in space: regional geopotential recovery from gravity gradiometry data *Inverse Problems: Principles And Applications in Geophysics, Technology, and Medicine. Proc. of the Int. Conf. (Potsdam, Germany, 30 August–3 September 1993)* (Berlin: Akademie) pp 60–75
[4] Dahlen F A and Simons F J 2008 Spectral estimation on a sphere in geophysics and cosmology *Geophys. J. Int.* **174** 774–807
[5] Engels J, Grafarend E, Keller W, Martinec Z, Sansò F and Vaníček P 1993 The geoid as an inverse problem to be regularized *Inverse Problems: Principles and Applications in Geophysics, Technology, and Medicine Proc. of the Int. Conf. (Potsdam, Germany, 30 August–3 September 1993)* (Berlin: Akademie) pp 122–66
[6] Etemadfard H and Hossainali M M 2016 Spherical Slepian as a new method for ionospheric modeling in arctic region *J. Atmos. Sol.-Terr. Phys.* **140** 10–5
[7] Freeden W, Gervens T and Schreiner M 1998 *Constructive Approximation on the Sphere with Applications to Geomathematics* (Oxford: Oxford University Press)
[8] Freeden W, Glockner O and Litzenberger R 1999 A general Hilbert space approach to wavelets and its application in geopotential determination *Numer. Funct. Anal. Optim.* **20** 853–79
[9] Freeden W, Michel V and Simons F J 2017 Spherical harmonics based special function systems and constructive approximation methods *Handbook of Mathematical Geodesy* ed W Freeden and M Z Nashed (Basel: Birkhäuser)
[10] Freeden W, Schneider F and Schreiner M 1997 Gradiometry—an inverse problem in modern satellite geodesy *Inverse Problems in Geophysical Applications. Proc. of the GAMM-SIAM Conf. (Yosemite, CA, USA, 16–9 December 1995)* (Philadelphia: SIAM) pp 179–239
[11] Gerhards C 2014 A combination of downward continuation and local approximation for harmonic potentials *Inverse Problems* **30** 085004
[12] Gutting M, Kretz B, Michel V and Telschow R 2017 Study on parameter choice methods for the RFMP with respect to downward continuation *Front. Appl. Math. Stat.* **3** 10
[13] Hielscher R and Schaeben H 2008 Multi-scale texture modeling *Math. Geosci.* **40** 63–82
[14] Huestis S P and Parker R L 1979 Upward and downward continuation as inverse problems *Geophys. J. R. Astron. Soc.* **57** 171–88
[15] Jahn K and Bokor N 2013 Solving the inverse problem of high numerical aperture focusing using vector Slepian harmonics and vector Slepian multipole fields *Opt. Commun.* **288** 13–6
[16] Jahn K and Bokor N 2014 Revisiting the concentration problem of vector fields within a spherical cap: a commuting differential operator solution *J. Fourier Anal. Appl.* **20** 421–51
[17] Khare K 2007 Sampling theorem, bandlimited integral kernels and inverse problems *Inverse Problems* **23** 1395–416
[18] Kusche J 2015 Time-variable gravity field and global deformation of the Earth *Handbook of Geomathematics* 2nd edn, ed W Freeden *et al* (Heidelberg: Springer) pp 321–38
[19] l'A Bromwich T J 1908 *An Introduction to the Theory of Infinite Series* (London: MacMillan and Co.)

[20] Laín Fernández N 2007 Optimally space-localized band-limited wavelets on $\mathbb{S}^{q-1}$ *J. Comput. Appl. Math.* **199** 68–79
[21] Laín Fernández N and Prestin J 2003 Localization of the spherical Gauss–Weierstrass kernel *Constructive Theory of Functions. Proc. of the Int. Conf. (Varna, Bulgaria, 19–23 June 2002)* (Sofia: DARBA) pp 267–74
[22] Landau H J and Pollak H O 1961 Prolate spheroidal wave functions, Fourier analysis and uncertainty—II *Bell Syst. Tech. J.* **40** 65–84
[23] Michel V 2002 A multiscale approximation for operator equations in separable Hilbert spaces—case study: reconstruction and description of the Earth's interior *Habilitation Thesis* Shaker, Aachen
[24] Michel V 2011 Optimally localized approximate identities on the 2-sphere *Numer. Funct. Anal. Opt.* **32** 877–903
[25] Michel V 2013 *Lectures on Constructive Approximation—Fourier, Spline, and Wavelet Methods on the Real Line, the Sphere, and the Ball* (New York: Birkhäuser) (https://doi.org/10.1007/978-0-8176-8403-7)
[26] Mitra P P and Maniar H 2006 Concentration maximization and local basis expansions (LBEX) for linear inverse problems *IEEE Trans. Biomed. Eng.* **53** 1775–82
[27] Müller C 1966 *Spherical Harmonics* (Berlin: Springer) (https://doi.org/10.1007/BFb0094775)
[28] Nakiboglu S M 1977 Solution of the downward continuation problem by the initial value method *Z. Vermess.wes.* **102** 248–50
[29] Plattner A and Simons F J 2017 Internal and external potential field estimation from regional vector data at varying satellite altitude *Geophys. J. Int.* **211** 207–38
[30] Schachtschneider R, Holschneider M and Mandea M 2010 Error distribution in regional inversion of potential field data *Geophys. J. Int.* **181** 1428–40
[31] Schneider F 1997 Inverse problems in satellite geodesy and their approximate solution by splines and wavelets *PhD Thesis* University of Kaiserslautern, Geomathematics Group. Shaker, Aachen
[32] Seibert K 2017 Thesis in preparation *PhD Thesis* University of Siegen, Department of Mathematics, Geomathematics Group
[33] Sharifi M A and Farzaneh S 2014 The spatio-spectral localization approach to modeling VTEC over the western part of the USA using GPS observations *Adv. SpaceRes.* **54** 908–16
[34] Simons F J 2010 Slepian functions and their use in signal estimation and spectral analysis *Handbook of Geomathematics* ed W Freeden *et al* (Heidelberg: Springer) pp 891–923
[35] Simons F J and Dahlen F A 2006 Spherical Slepian functions and the polar gap in geodesy *Geophys. J. Int.* **166** 1039–61
[36] Simons F J, Dahlen F A and Wieczorek M A 2006 Spatiospectral concentration on a sphere *SIAM Rev.* **48** 504–36
[37] Simons F J, Loris I, Nolet G, Daubechies I C, Voronin S, Judd J S, Vetter P A, Charléty J and Vonesch C 2011 Solving or resolving global tomographic models with spherical wavelets, and the scale and sparsity of seismic heterogeneity *Geophys. J. Int.* **187** 969–88
[38] Slepian D 1964 Prolate spheroidal wave functions, Fourier analysis and uncertainty—IV: extensions to many dimensions; generalized prolate spheroidal functions *Bell Syst. Tech. J.* **43** 3009–57
[39] Slepian D and Pollak H O 1961 Prolate spheroidal wave functions, Fourier analysis and uncertainty—I *Bell Syst. Tech. J.* **40** 43–63
[40] Starck J L, Murtagh F and Fadili J M 2015 *Sparse Image and Signal Processing. Wavelets and Related Geometric Multiscale Analysis* 2nd updated edn (Cambridge: Cambridge University Press)
[41] Telschow R 2014 An orthogonal matching pursuit for the regularization of spherical inverse problems *PhD Thesis* University of Siegen, Department of Mathematics, Geomathematics Group
[42] Tsuboi C 1961 Upward and downward continuation of gravity values based on the cylindrical co-ordinate system *Proc. Japan Acad.* **37** 37–41
[43] Vareschi T 2014 Application of second generation wavelets to blind spherical deconvolution *J. Multivariate Anal.* **124** 398–417
[44] Wieczorek M A and Simons F J 2005 Localized spectral analysis on the sphere *Geophys. J. Int.* **162** 655–75
[45] Wieczorek M A and Simons F J 2007 Minimum-variance spectral analysis on the sphere *J. Fourier Anal. Appl.* **13** 665–92
[46] Xu P 1998 Truncated SVD methods for discrete linear ill-posed problems *Geophys. J. Int.* **135** 505–14